An individual-based model study of anchovy early life history in the northern Humboldt Current system

Timothée Brochier [a,*], Christophe Lett [b], Jorge Tam [c], Pierre Fréon [a], François Colas [c,1], Patricia Ayón [c]

[a] Institut de Recherche pour le Développement, UR ECO-UP, CRHMT Centre de Recherche Halieutique Méditerranéenne et Tropicale, Avenue Jean Monnet, BP 171 34203 Sète Cedex, France
[b] Institut de Recherche pour le Développement, UR ECO-UP, University of Cape Town, Oceanography Department, Rondebosch 7701, South Africa
[c] Instituto del Mar del Peru (IMARPE), Esquina Gamarra y General Valle S/N Chucuito Callao, Peru

ARTICLE INFO

ABSTRACT

We used an individual-based model of anchovy (Engraulis ringens) early life history coupled with hydrodynamic outputs from the regional oceanic modeling system (ROMS) to investigate the factors driving variability in egg and larval survival rates in the northern Humboldt upwelling region off Peru. Individuals were released within a coastal area and followed for a period of 30 days. Those that were still in the coastal area at that time were considered as retained. We investigated the spatial and temporal variability in the release locations of the individuals retained, and compared these to observed egg concentration patterns reconstructed from a 40-year period of monitoring. A first set of simulations using passive particles to represent anchovy eggs and larvae revealed a large sensitivity of the results to the initial vertical distribution of particles. We then conducted two additional sets of simulations that included the effect of egg buoyancy, larval vertical swimming behavior and lethal temperature. We obtained (1) maximal coastal retention close to the surface in winter and in deeper layers in summer, (2) a large influence of egg buoyancy and of larval vertical behavior on coastal retention in all seasons, (3) a partial match between dates and locations of enhanced retention and observed egg concentration patterns and (4) a low effect of lethal temperature on survival except when associated with high egg density. The model suggests that an optimal temporal spawning pattern for maximizing coastal retention would have two maximums, the most significant in austral winter and the second in summer. This pattern agrees roughly with observed spawning seasonality, but with temporal discrepancy of about two months in the peaks of both series. Spatially, we obtained higher retention from 10 S to 20 S, whereas the observed maximum egg concentration was located between 6°S and 14°S. Among the three sets of simulations, the one taking into account larval vertical swimming behavior lead to the best match with the data.

© 2008 Elsevier Ltd. All rights reserved.

1. Introduction

Upwelling ecosystems support large populations of small pelagic fish, particularly clupeoids like anchovy and sardine (Fréon et al., 2006). These species are believed to control the trophic dynamics of these systems (Cury et al., 2000) and are often exploited by industrial and artisanal fisheries (Fréon et al., 2005). High levels of recruitment variability make anchovy and sardine stocks particularly difficult to manage (Jacobson et al., 2001). As these fish are short-lived and often heavily exploited the bulk of the biomass comes from one (anchovy) to three (sardine) year-classes. Consequently, fluctuations in recruitment success translate rapidly into fluctuations in population sizes. It is generally accepted that recruitment dependence on the spawning biomass is low, except at very low levels of parental biomass (Fogarty, 1993; Myers, 1998; Myers et al., 1999), and that it depends mainly on survival during the first life stages. Survival is thought to be mainly mediated by environmental conditions rather than by density-dependent processes. Environmental conditions which could influence the survival of the early life stages have been well described (Bakun, 1996; Cury and Roy, 1989; Lasker, 1985). However, forecasting environmentally driven fluctuations in recruitment remains problematic.

The Humboldt Current system is one of the world's major eastern boundary current upwelling systems, and it currently

* Corresponding author.
E-mail addresses: timothee.brochier@ifremer.fr (T. Brochier), christophe.lett@ird.fr (C. Lett), jtam@imarpe.gob.pe (J. Tam), Pierre.Freon@ifremer.fr (P. Fréon), francois@atmos.ucla.edu (F. Colas), payon@imarpe.gob.pe (P. Ayón).
[1] Present address: Institute of Geophysics and Planetary Physics (IGPP), University of California Los Angeles, Los Angeles, CA, USA.

sustains a huge stock of anchovy (*Engraulis ringens*), also called anchoveta, that is exploited by thousands of purse-seiners whose annual landing exceeds 5 million tons (Ñiquen and Fréon, 2006). This stock has been monitored since the 1960s by the Peruvian institute IMARPE, providing extensive information on spawning dates and areas despite their large variability (Santander, 1981; Senocak et al., 1989). Anchovy reproduction usually displays two annual peaks, with a major spawning in late winter (August–September) and a secondary spawning in summer (February–March). On average, the winter spawning season is much more intense than the summer one, and the main spawning area is located between 6°S and 14°S. However, inside this large area spawning is both spatially and temporally very irregular. Muck (1989) found a strong negative relationship between the proportion of mature females and temperature but the data were not spatialized. Another study suggested that larvae survived better off the northern coast of Peru during the austral winter season when motile (swimming) algae are available as food (Walsh et al., 1980). Understanding the factors driving anchovy spawning date and location and their impact on eggs and larvae is a key question for local fisheries management.

Realistic numerical hydrodynamic models at a regional scale have recently become available as computational power has rapidly increased over the last decade (Haidvogel and Beckmann, 1998). These models have increasingly been coupled with individual-based models to study the dynamics of early life stages of marine species (Miller, 2007; Werner et al., 2001) and particularly small pelagic fish (Lett et al., in press). Recently, a climatological hydrodynamic simulation of the northern Humboldt upwelling region at a relatively high resolution (1/9°) has been developed and validated (Penven et al., 2005). Lett et al. (2007a) used it to build putative maps of Bakun's triad processes (concentration, retention and enrichment, Bakun, 1996). They showed that the area of largest concentration of anchovy eggs matched the area of optimal simulated enrichment and retention, and that maximum retention rates occurred in summer while enrichment was stronger in winter. Although their results could explain some of the significant anchovy spawning patterns, they could not explain others, like the bimodal seasonal distribution of anchovy egg production usually observed in Peru. In this paper, the same climatological hydrodynamic simulation was used but with a different (and complementary) approach. Instead of mapping separately Bakun's triad elements, we studied the functional impact of anchovy spawning period, vertical egg and larval movements (buoyancy and swimming), and mortality on anchovy retention, following the methodology described by Mullon et al. (2003). We compared the model output with observed data on spawning patterns, following the pattern-oriented modelling (Grimm et al., 2005) approach. Field egg concentration of anchovy eggs as surveyed by IMARPE were used as a proxy for spawning location and period.

It is generally accepted that clupeoids maximize egg and larval retention by spawning in favorable areas (Bakun, 1996), and there is no evidence of the Peruvian anchovy being an exception. Therefore, one of the questions addressed in this paper is whether it is possible, with a simple condition of larval retention in the phytoplankton-rich coastal area, to model features of the observed spawning behavior. In other words, does the Peruvian anchovy spawning maximize the retention condition? We also investigated the impact of egg buoyancy and larval swimming on retention, using different vertical swimming behaviors such as diurnal vertical migration (DVM) and ontogenic migration. Finally, being in an area where the presence of upwelled waters leads to large temperature variations, we also tested different lethal temperatures to analyze how they might interact with other factors to modulate retention.

2. Methods

2.1. The model

The individual-based model (IBM) description below follows the overview-design-details (ODD) protocol for describing individual- and agent-based models (Grimm et al., 2006; Grimm and Railsback, 2005) and consists of six subsections below. The first two subsections provide an overview, the fourth explains general concepts underlying the model design, and the remaining three subsections provide details. The present model is a version of a modeling tool called Ichthyop (Lett et al., 2008) that can be downloaded from http://www.eco-up.ird.fr/projects/ichthyop/.

2.1.1. Purpose

We used a coupled model of transport and survival of anchovy early life stages to assess coastal retention rates depending on spawning tactics, and compared optimized results with the observed reproduction patterns. We also used the model to investigate the relative importance of environmental and behavioral factors on retention.

2.1.2. State variables and scales

The model is composed of virtual individuals and their marine physical environment. Individuals were characterized by the state variables: age (in days), location (in three dimensions, longitude, latitude and depth), life stage (egg or larva) and status (alive or dead). The environment was characterized by three-dimensional fields of state variables: water velocity (in m s^{-1}), temperature (in °C) and salinity (PSU).

Environmental conditions were provided by archived simulations of the regional oceanic modeling system (ROMS) (Shchepetkin and McWilliams, 2005) configured for the Peruvian region (Penven et al., 2005). The grid extends from 5°N to 22°S and from 70°W to 92°W with a horizontal resolution of 1/9°. Since ROMS uses terrain-following curvilinear coordinates with 32 layers in this configuration, the vertical resolution ranges from 30 cm to 6.25 m at the surface layer and from 31 cm to 1086 m at the bottom layer. To investigate the seasonal variability of the environment we used a simulation forced with monthly climatological atmospheric fluxes and boundary conditions. Penven et al. (2005) validated the modeled seasonal cycle. Since the mesoscale environment is variable in different simulation years (with the same climatological forcing) due to intrinsic model variability (Batteen, 1997; Marchesiello et al., 2003), a set of three years was chosen randomly among those used by Penven et al. (2005). Water velocity, temperature and salinity fields were averaged and stored every two days. These fields were interpolated in time and space in the IBM to determine values of the environmental state variables at any individual location every two hours. Every simulation lasted for 30 days.

2.1.3. Process overview and scheduling

Virtual eggs were released in the environment following a determined spatial (area, depth and patchiness) and temporal (month, duration and frequency) spawning strategy that constituted the initial conditions (see Sections 2.1.5 and 2.1.6.1). Once released, each egg or larva within each time step was moved, tested for mortality and finally for retention (see Sections 2.1.6.2–2.1.6.4). Depending on the type of simulation, the movement was a passive Lagrangian transport with or without addition of a buoyancy scheme for eggs, or a vertical swimming behavior scheme for larvae.

2.1.4. Design concepts
2.1.4.1. Stochasticity. The release location for each individual was chosen randomly within the specified spawning areas. It aimed

at simulating patchy or uniform distributions depending on a patchiness parameter (see Section 2.1.6.1). Instead of testing a repetition effect that largely depended on the initial number of released particles, as did Mullon et al. (2003), the number of individuals chosen was large enough (3000 individuals) to avoid effects due to the random initial location. Therefore only one simulation for each set of parameters was necessary.

2.1.4.2. Observation. A series of simulations were run with different pre-defined sets of parameters. For each simulation the proportion of individuals retained within the coastal area was calculated. We then performed a variance analysis on the proportion of retained individuals. We also investigated the spatial and temporal variability in the release locations of the individuals retained, and compared these to observed egg concentration patterns reconstructed from a 40-year period of monitoring.

2.1.5. Initialization

In each simulation 3000 particles representing virtual eggs were released in the spawning area at the beginning of each month. The spawning area extended from 2°S to 20°S, and from the coast to the 3000 m isobath, which roughly corresponds to the zone of maximum chlorophyll concentrations (Fig. 1). The initial conditions of virtual spawning were defined by year (in the climatological series), month, spawning frequency, area, patchiness and depth (see Section 2.1.6.1). For each simulation, a set of individual characteristics was also chosen: lethal temperature, egg buoyancy and vertical migration behavior (see Sections 2.1.6.2 and 2.1.6.3).

2.1.6. Submodels

2.1.6.1. Spawning strategy. The spawning strategy was defined by the (virtual) spawning area, depth, time, duration, frequency and patchiness. The spawning area was a set of sub-areas covering the coastal zone previously defined (see Section 2.1.5). These sub-areas were defined by three bathymetric intervals (0–100 m,
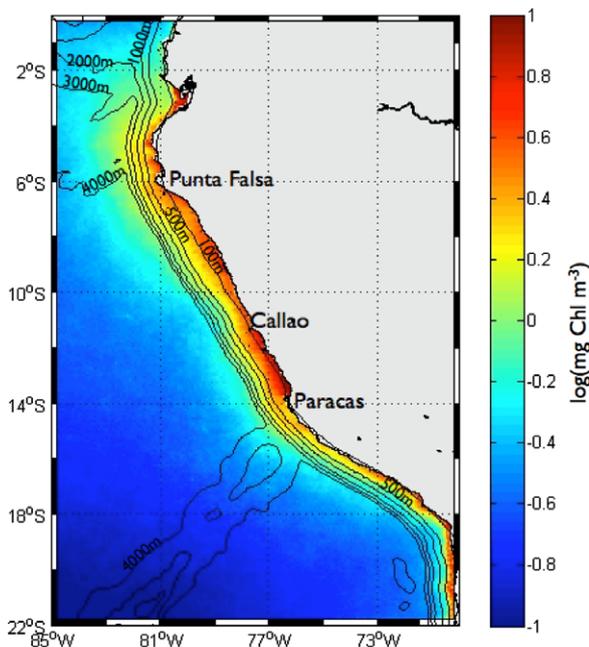
100–500 m and 500–3000 m) and nine latitudes (every two degrees from 2°S to 20°S). Depth of spawning was defined by an interval (upper and lower depth levels, in m). Spawning time was defined by year and month. Spawning frequency and spawning patchiness were parameters used to set the time and space distribution of the released particles. Spawning frequency was the number of times virtual eggs were released within the spawning period (one month). For this parameter we used values of 1, 3 and 5 to set that all virtual eggs (3000) were released on day 0, 1/3 of them (1000) on days 0, 10 and 20, or 1/5 (600) on days 0, 6, 12, 18 and 24. Spawning patchiness indicated the number of particles released around the same location (±1 m for depth, ±1 1/9° for longitude and latitude). For this parameter we used values of 1, 10 and 100. This last value, for example, indicates that the 3000 particles were released by groups of 100 around any location, i.e., the distribution of particles was patchy, with 30 patches of 100 particles. Locations were randomly chosen within the spawning area.

2.1.6.2. Movement. Depending on the type of simulation, the movement was purely Lagrangian (passive), with buoyancy for eggs or with vertical swimming behavior for larvae (Eq. (1)). Egg buoyancy was calculated as a function of egg density and water density, the latter being calculated as a function of water temperature and salinity (see Parada et al., 2003 for details). The buoyancy scheme was only applied before hatching, i.e., during the first two days after spawning, as suggested by laboratory experiments (Ware et al., 1980). Depending on the type of simulation, the vertical swimming behavior consisted in a diurnal vertical migration (DVM) between two fixed depths (scenario 1) or in maintaining fixed depths at 1, 15 or 30 m (scenario 2, 3 and 4, respectively). The larval vertical swimming scheme was applied 4 days after hatching, i.e., from day 6, roughly corresponding to the time of complete yolk resorption (Ware et al., 1980). In scenario 1 the vertical swimming velocity was an age-dependent function derived from an age-length relationship (Castro and Hernández, 2000) and a length–velocity relationship (Hunter, 1977). The resulting age–velocity relationship was linear for the first month (Eq. (2)). Anchovy larvae swam approximately a distance equal to their size in one second (Hunter, 1977). We considered that this velocity could be applied for vertical migrations

$$
\begin{aligned}
x(t + \Delta t) &= x(t) + V_u \cdot \Delta t, \\
y(t + \Delta t) &= y(t) + V_v \cdot \Delta t, \\
z(t + \Delta t) &= z(t) + (V_z + V_{buoy}(a) + B \cdot V_{swim}(a)) \cdot \Delta t,
\end{aligned}
\tag{1}
$$

(x, y, z) = individual's position; a = individual's age (days since spawning); t = time, $V_{u,v,z}$ = current velocity along u, v or z axis, $V_{buoy}(a)$ = buoyancy velocity depending on egg and water density, $V_{swim}(a)$ = swimming velocity in cm s^{-1}, B = vertical migration behavior ± 1 depending on depth and time for DVM.

$$
\begin{aligned}
&\text{for } a \leqslant 6 : V_{swim} = 0, \\
&\text{for } a > 6 : V_{swim} = 0.1 + 0.08 \cdot (a - 6),
\end{aligned}
\tag{2}
$$

a is the time since spawning in days and V_{swim} is the swimming velocity in cm s^{-1}.

2.1.6.3. Mortality. Mortality was temperature-dependent: virtual eggs and larvae died when they were exposed to temperature below a pre-defined threshold value. Although there are few data concerning the lethal temperature for anchovy larvae in Peru, larval survival is known to be strongly dependent on length at hatching, which is usually optimal at intermediate temperature in a given environment (Llanos-Rivera and Castro, 2006; Pauly and Soriano, 1989). Off Peru, the observed temperature range for adults anchovy spawning is 14–21 °C (Jarre et al., 1991),

Fig. 1. Superficial chlorophyll *a* concentration annual mean, over the period 1997–2003 (SeaWiFS) superposed with isobaths 100, 500, 1000, 2000, 3000 and 4000 m. The higher chlorophyll *a* concentration is above the continental shelf. Source: ocean Color Web: oceancolor.gsfc.nasa.gov – processing: interanual means – IRD (D. Dagorne).

without evidence of temperature selection for spawning (Bertrand et al., 2004). Here we tested the impact of three different arbitrary lethal temperature (12, 14 and 16 °C). These values were selected after preliminary tests in order to obtain contrasted results.

2.1.6.4. Coastal retention. Individuals were considered as retained when they were alive and still in the coastal area after the drift period. We make the generally accepted assumption that the variability of the recruitment is highly correlated to this retention (Bakun, 1996). Based on *in situ* observations (e.g, Ayón, 2004), the coastal area was the same as the spawning area, i.e., the area where high chlorophyll concentrations were observed (Fig. 1). For the drift period we used the "horizontal-current independent age", i.e., the age at which larvae can swim fast enough to influence their horizontal motion within the current field. The Peruvian anchovy larval stage duration is about 1.5 months, after which larvae metamorphose into juveniles and recruits (i.e., fish of 37.5–47.5 mm) at 3 months (Palomares et al., 1987). The age-velocity relationship previously described indicated one month-old larvae can swim >2 cm s^{-1}, which might be sufficient to influence motion within currents in the coastal area which typically flow <10 cm s^{-1} (Fig. 10). Therefore we set the drifting time to 30 days after spawning.

Table 1
Parameters tested in each set of simulation.

	Sim I	Sim II	Sim III
Latitude	−2–4 °S, 4–6 °S, 6–8 °S, 8–10 °S, 10–12 °S, 12–14 °S, 14–16 °S, 16–18 °S, 18–20 °S—		
Bathymetry	−0–100 m, 100–500 m, 500–3000 m—		
Month	—Every months—		
Year	3	1	1
Depth of spawning	0–15 m, 15–30 m, 30–45 m	0–50 m	0–50 m
Frequency	1, 3, 5	1	1
Patchiness	1, 10, 100	1	1
Egg density	No	1.023, 1.024, 1.025, 1.026, 1.027	No
Lethal temperature	No	12, 14, 16 °C	No
Vertical swimming behavior	No	No	DVM 0–30 m, Target depth 1 m, 15 m, 30 m

2.2. Simulation experiments, sensitivity analysis and pattern analysis

We performed three sets of simulations (Table 1), which tested the following factors: (1) Considering only Lagrangian drift, the effects of different spawning strategies (location, date, time, depth, etc.) on retention pattern (Simulation I); (2) The effects of varying egg buoyancy (Simulation II) and larval swimming (Simulation III) on retention pattern.

Because our modeling design was similar to that of many experiments, we chose to perform analysis of variance (ANOVA) using retention rates as the dependent variable, the different tested effects (egg density, lethal temperature, spatial and temporal effects) and their first degree interactions as fixed factors. We checked that the error distribution was close to a Gaussian distribution and that the assumption of variance homogeneity was fulfilled. Because the spatio-temporal autocorrelation in the simulated data resulted in an overestimation of the number of degrees of freedom of the ANOVA, and hence of the significance level of the factors, we chose arbitrarily 2% for the explained variance as threshold to discuss the effect of the factors.

Finally, we compared retention spatial and seasonal patterns obtained with the IBM with field observations of anchovy egg concentrations. We derived an egg-distribution climatology with field data from 1961 to 2004. Considering that this observed distribution reflected the average spawning pattern, we compared it with the retention patterns resulting from Simulation III, with a target depth of 15 m, which seems the most realistic in terms of egg and larval depth regulation. If the natural selection has maximized retention within the chlorophyll-rich coastal area for Peruvian anchovy as modeled here, then one would expect observed spawning and retention patterns to be similar in time and space.

3. Results

3.1. Sensitivity analysis

3.1.1. Simulation I

Factors included in the analysis of variance of the simulated retention values were (Table 2): date (year and month) of spawning, area (latitude and bathymetry) and depth of spawning, spawning frequency and patchiness. Spawning depth explained more than 20% of the total variance in the retention values, followed by latitude (7%) and bathymetry (4%). Year, spawning frequency and patchiness explained very little of the variance. On average,

Table 2
ANOVA of IBM's output for Simulation I show the relative importance of each factor on the variation of the coastal retention rate.

	Df	Sum Sq	Mean Sq	*F* value	% Expl.	Pr(>*F*)
Depth	2	4,074,222	2,037,111	8043.3	22.7	<2.2e−16
Latitude	8	1,290,999	161,375	637.2	7.2	<2.2e−16
Bathymetry	2	694,725	347,362	1371.5	3.9	<2.2e−16
Month	11	250,306	22,755	89.8	1.4	<2.2e−16
Year	2	11,485	5743	22.7	0.1	1.45e−10
Patchiness	2	2490	1245	4.9	0.0	0.0073315
Frequency	2	387	194	0.8	0.0	0.4657411
Depth×latitude	16	385,742	24,109	95.2	2.2	<2.2e−16
Depth×bathymetry	4	71,194	17,798	70.3	0.4	<2.2e−16
Depth×month	22	1,040,158	47,280	186.7	5.8	<2.2e−16
Depth×year	4	5498	1375	5.4	0.0	0.0002299
Latitude×bathymetry	15	1,092,955	72,864	287.7	6.1	<2.2e−16
Latitude×month	88	1,827,175	20,763	82.0	10.2	<2.2e−16
Latitude×year	16	42,677	2667	10.5	0.2	<2.2e−16
Bathymetry×month	22	507,748	23,079	91.1	2.8	<2.2e−16
Bathymetry×year	4	5542	1386	5.5	0.0	0.0002124
Month×year	22	40,613	1846	7.3	0.2	<2.2e−16
Residuals	25,981	6,580,173	253		36.7	
Total		17,924,089			100.0	

retention increased with spawning depth, from ~20% for a spawning at 0–15 m to ~45% at 30–45 m. Retention was higher over the continental shelf (~40% for particles released from the coast to the 100 m isobath) and decreased offshore (~20% for particles released in the area between the 500 m and 3000 m isobaths). Five interactions between factors explained more than 2% of the variability but with high degrees of freedom and therefore relatively low mean square values (Table 2). The most significant was the month×latitude interaction. High (>40%) retention values were found from 8°S to 14°S from June to October. Low (<20%) values were observed all year round from 2°S to 6°S (Fig. 2). The month×depth interaction was observed together with the month×bathymetry interaction (Fig. 3). For the 30–45 m depth level, retention values peaked during late spring (November–January) and were minimal in winter
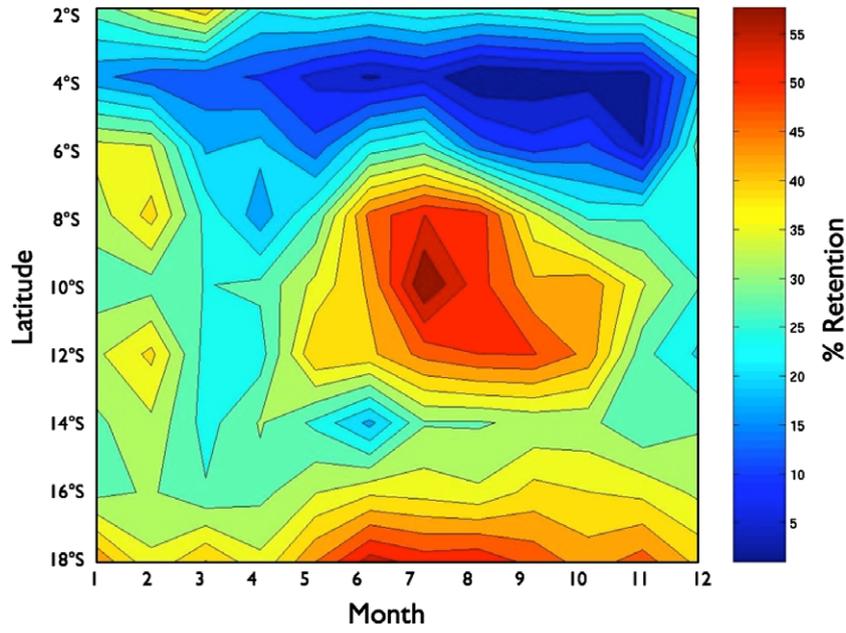
Fig. 2. Hovmuller diagram of the retention rates (Simulation I). The maximum of retention does not occur at the same place in winter and summer.
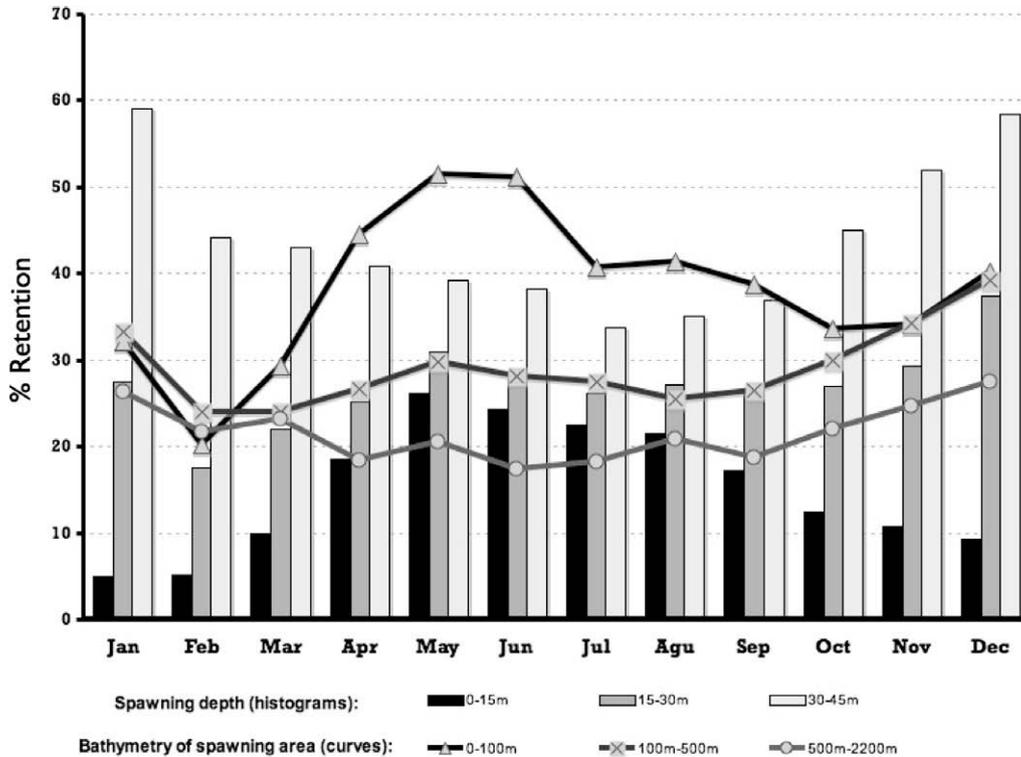
Fig. 3. Monthly retention rates (Simulation I). Histograms: particles released at three different depth ranges (0–15, 15–30 and 30–45 m). Curves: particles released at different position above the continental shelf: coast to isobaths 100 m; 100–500 m; 500–3000 m. This figure shows (1) the opposite seasonal pattern of retention for the 0–15 m and the 30–45 m cape, and (2) the higher retention rate in spring and summer over the shallow shelf (0–100 m).

(June–September), while the opposite seasonal pattern was obtained for the 0–15 m level. Maximum values of retention were obtained in fall (May–June) for particles released close to the coast and during late spring (November–January) for particles released further offshore. Because spawning depth was identified as the most sensitive parameter, we conducted two additional sets of simulations which included processes that affected the vertical distribution of eggs and larvae.

3.1.2. Simulation II

We tested the effect of different values of egg buoyancy (egg densities of 1.023, 1.024, 1.025, 1.026 and 1.027 g cm^{-3}) and of lethal temperature (12, 14 and 16 °C) on the simulated retention. We modeled different values only for the single parameters that were found as the most sensitive in the previous simulation, i.e., month, latitude and bathymetry, but held the remaining factors constant (Table 1). The spawning depth was set between 0 and 50 m. ANOVA on the retention values (Table 3) showed that egg buoyancy strongly contributed to the variability in retention values (~30% of the variance) while the lethal temperature contributed only 7.6%. Increased egg density in the range 1.024–1.026 g cm^{-3} strongly increased retention values (Fig. 4). Temperature-dependent mortality was only significant for the highest density class (1.027 g cm^{-3}). A high lethal temperature threshold was detrimental in this case (Fig. 4) suggesting that virtual eggs sank into low

temperature waters before hatching. To confirm these hypothesis we analyzed the vertical distribution (averaged over the entire coastal area and over the year) after 2 days of transport for eggs randomly released between 0 and 50 m. For density values of 1.023 and 1.024 g cm^{-3}, eggs concentrated close to the surface. For a density of 1.025 g cm^{-3} they remained mainly between 0 and 50 m, while for larger values, eggs sank rapidly, reaching waters deeper than 150 m for a density of 1.027 g cm^{-3} (not shown). The large mortality observed for an egg density of 1.027 g cm^{-3} was consistent with the annual mean depth of the lethal 16 °C isotherm between 7°S and 13°S from the coast to 500 km offshore, which was about 150 m in the hydrodynamic model (Penven et al., 2005). The density×month interaction (Fig. 5) showed maximum retention in winter (June–August) for densities of 1.023 and 1.024 g cm^{-3}. For larger values there were two maxima, one in winter (June–August) and the other in summer (December–February). The density×bathymetry interaction (Fig. 4) showed that for a egg density of 1.025 g cm^{-3} and higher the largest retention values were obtained for spawning grounds between 100 and 500 m, while for lower values of density retention was maximum for the coastal spawning area. Finally, the density×latitude interaction indicated latitudinal variability of retention values for low density values (1.023 and 1.024 g cm^{-3}). As these densities were the most superficial, this was certainly due to alongshore variations of the upwelling strength.

Table 3
ANOVA of IBM's output for Simulation II show the relative importance of each factor on the variation of the coastal retention rate.

	Df	Sum Sq	Mean Sq	F value	% Expl.	Pr(>F)
Density	4	1,235,548	308,887	1293.86	29.08	<2.2e−16
Lethal temperature	2	323,280	161,640	677.07	7.61	<2.2e−16
Latitude	8	290,444	36,306	152.08	6.84	<2.2e−16
Month	11	56,661	5151	21.58	1.33	<2.2e−16
Bathymetry	2	51,086	25,543	106.99	1.20	<2.2e−16
Density×lethal temperature	8	369,698	46,212	193.57	8.70	<2.2e−16
Density×latitude	32	323,531	10,110	42.35	7.62	<2.2e−16
Density×month	44	121,762	2767	11.59	2.87	<2.2e−16
Density×bathymetry	8	74,890	9361	39.21	1.76	<2.2e−16
Lethal temperature×latitude	16	26,367	1648	6.90	0.62	6.21e−16
Lethal temperature×month	22	2726	124	0.52	0.06	0.968
Lethal temperature×bathymetry	4	17,465	4366	18.29	0.41	6.51e−15
Latitude×month	88	161,927	1840	7.71	3.81	<2.2e−16
Latitude×bathymetry	15	107,884	7192	30.13	2.54	<2.2e−16
Month×bathymetry	22	36,449	1657	6.94	0.86	<2.2e−16
Residuals	4392	1,048,514	239		24.68	
Total		42,48,232			100.00	
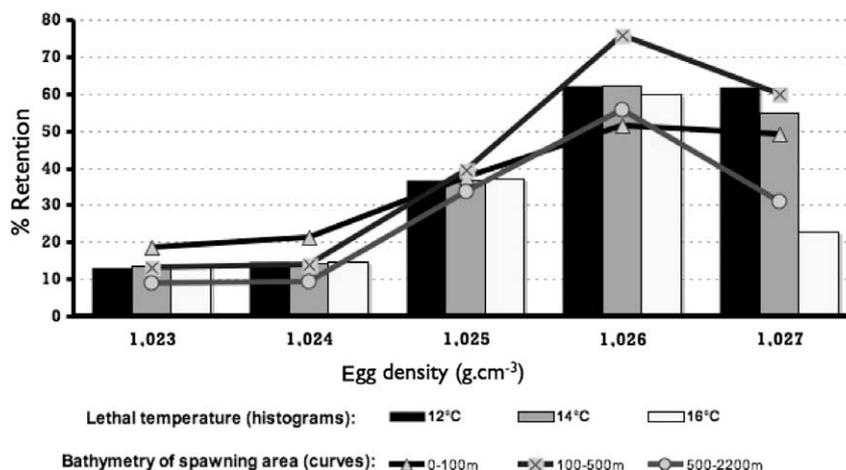
Fig. 4. Retention rates for four different egg buoyancy (Simulation II). Histograms: egg lethal temperatures of 12, 14 and 16 °C; Curves: spawning from coast to isobaths 100 m; 100–500 m; 500–3000 m. Retention increases when buoyancy decreases, but lethal temperature then becomes limitant.
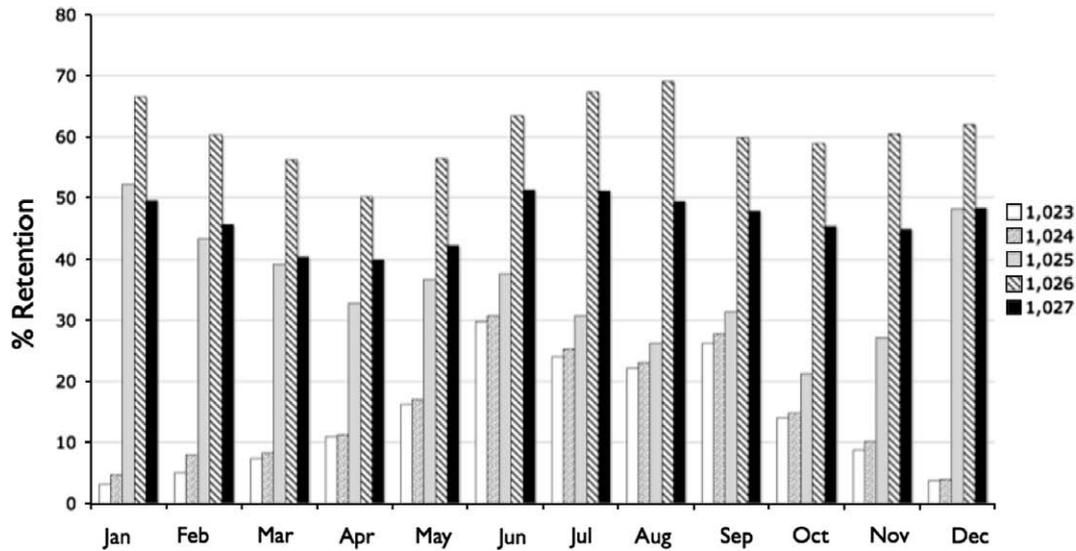
Fig. 5. Monthly retention rate for four egg buoyancy (Simulation II). Heavy eggs (>1.025 g cm^{-3}) retention have two seasonal maxima while light eggs (<1.025 g cm^{-3}) have only one maximum.

3.1.3. Simulation III

Simulated larvae were given depth-regulatory behavior: (1) a diurnal vertical migration (DVM) between 1 and 30 m, or a target depth of (2) 1 m, (3) 15 m, (4) 30 m. In this simulation vertical behavior was the main factor contributing to retention variability (~19%), followed by the latitude (~18%), month (~5%) and bathymetry (~4%) factors (Table 4). On average the simulated retention values increased with the target depth from ~30% (at 1 m) to ~55% (at 30 m). The DVM scenario gave an average retention value of ~40%, slightly lower than the scenario using a target depth of 15 m. The vertical behavior×month interaction explained a substantial part of the variance (~8%) but again with a high number of degrees of freedom (33). The retention patterns also changed much with bathymetry. For the coastal area (until 100 m depth) the retention values were maximal during winter for all vertical behavior scenarios. More offshore the scenarios using a target depth of 1 or 30 m showed opposite retention patterns, while the DVM scenario and the 15 m depth one showed two maximums of retention, one during winter and one during summer (Fig. 6).

3.2. Pattern analysis

3.2.1. Seasonal pattern

The two peaks observed in the mean seasonal distribution of collected anchovy eggs could be compared with the two peaks obtained for retention in the simulation using vertical swimming behavior (Simulation III) and a target depth of 15 m with a spawning over the whole area (0–3000 m), or only over the shelf (0–100 m). Although the correlation between maximum observed spawning and enhanced simulated retention was not precise, the main seasonal variation pattern was retrieved (Fig. 7). For spawning over the whole domain, the summer peak was larger than the winter one. By contrast, for spawning over the shelf only, where the majority of the eggs are actually spawned, the winter peak was larger. In both cases a temporal discrepancy of about two months was observed with the field data peaks (for technical reasons the hydrodynamic model started on January 15th so that the temporal shift was actually one month and a half).

3.2.2. Spatial pattern

Field observations indicated that anchovy eggs were found mainly between 6°S and 14°S (Fig. 8). In the areas 6°S–10°S and 14°S–20°S anomalies of egg concentrations and anomalies of retention values were opposite. At 6°S–10°S, the observed egg concentration was significant despite relatively low retention simulated by the model. In contrast, from 14°S to 20°S, field data indicated relatively low egg concentrations despite a high simulated retention (Fig. 8). However, the hydrodynamic model in that region did not reproduce properly the Paracas upwelling cell (Penven et al., 2005), which might lead to an overestimation of retention there.

Table 4
ANOVA of IBM's output for Simulation III show the relative importance of each factor on the variation of the coastal retention rate.

	Df	Sum Sq	Mean Sq	F value	% Expl.	Pr(>F)
Vertical_behavior	3	73,278	24,426	301.13	19.29	<2.2e−16
Latitude	8	70,184	8773	108.15	18.47	<2.2e−16
Month	11	17,687	1608	19.82	4.66	<2.2e−16
Bathymetry	2	15,911	7956	98.08	4.19	<2.2e−16
Vertical_behavior×latitude	24	4994	208	2.57	1.31	5.53E−05
Vertical_behavior×month	33	31,869	966	11.91	8.39	<2.2e−16
Vertical_behavior×bathymetry	6	1711	285	3.51	0.45	0.0019
Latitude×month	88	53,371	606	7.48	14.05	<2.2e−16
Latitude×bathymetry	15	10,942	729	8.99	2.88	<2.2e−16
Month×bathymetry	22	16,009	728	8.97	4.21	<2.2e−16
Residuals	1035	83,955	81		22.10	
Total		379,911			100.00	
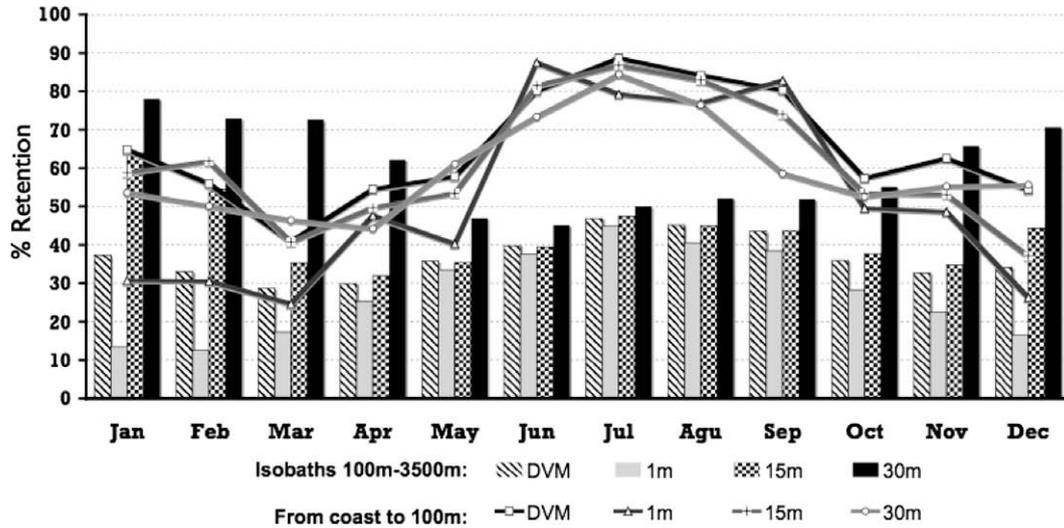
Fig. 6. Monthly retention rate for different scenarios of larval vertical migration (Simulation III). Histograms: eggs released from isobaths 100 m to 3500 m. Curves: eggs released from coast to isobath 100 m. Retention is constant in summer for any vertical swimming behavior while in winter retention is lower for larvae migrating to the near surface and higher for larvae migrating to 30 m depth. For eggs released over the shallow shelf (<100 m), the retention is much stronger in winter.
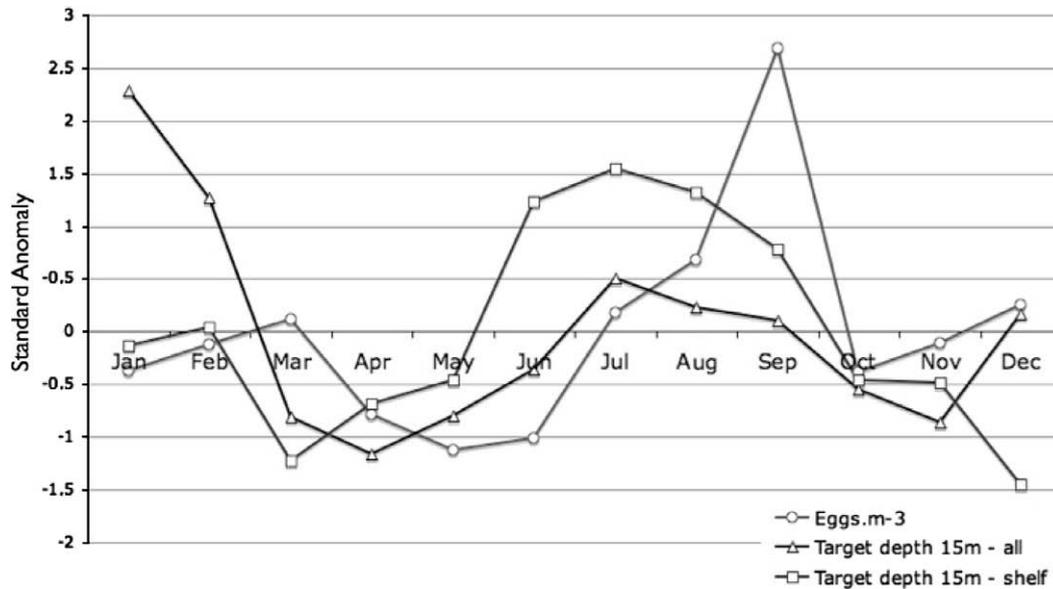
Fig. 7. Standard anomalies of the mean monthly anchovy egg concentrations and the retention for larvae migrating to 15 m depth (Simulation III) released (1) from coast to isobath 3000 m (curve with triangles), (2) from coast to isobath 100 m (curve with squares). The relative importance of the summer and winter peaks of retention depends on whether spawning was sets over the shelf or not.
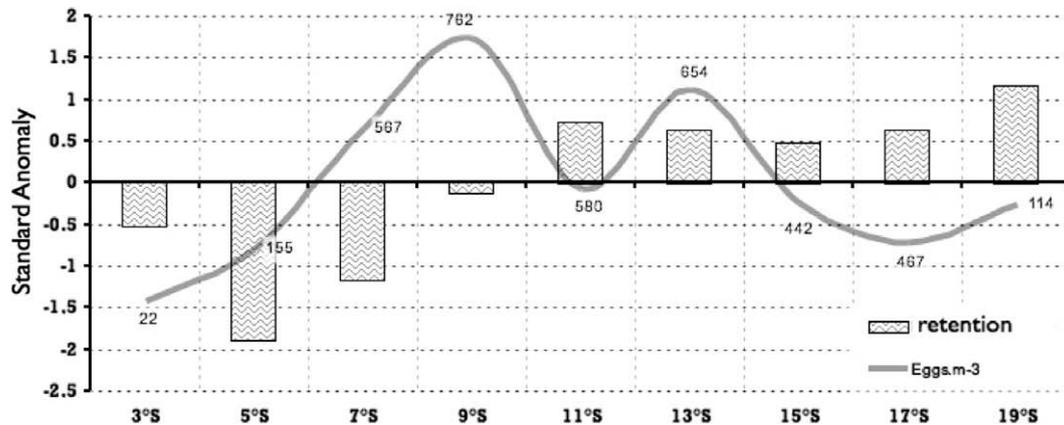
Fig. 8. Spatial comparison between retention (Simulation III) and eggs concentration standardized anomalies. The numbers near the curve indicate the number of data available (square of 1/10° latitude × 1/10° longitude where there is data).
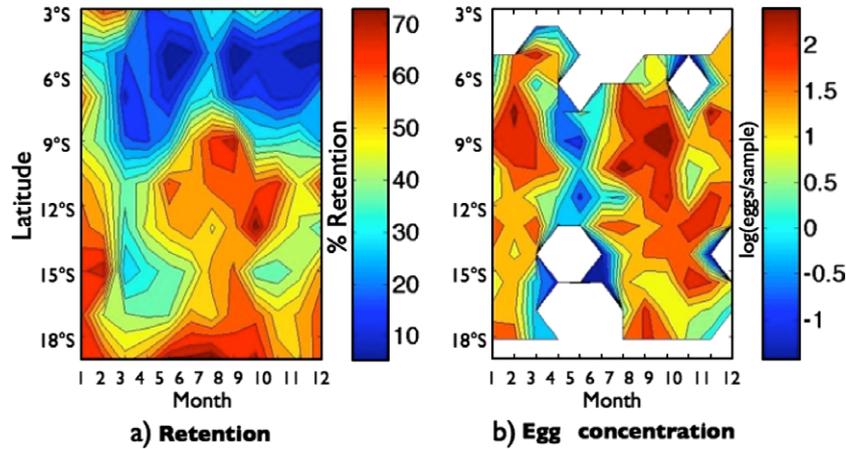
Fig. 9. Spatio-temporal egg concentrations and retention patterns. (a) Hovmuller diagram of retention (Simulation III, target depth 15 m). (b) Hovmuller diagram of anchovy eggs concentration (blank indicates no sufficient data).
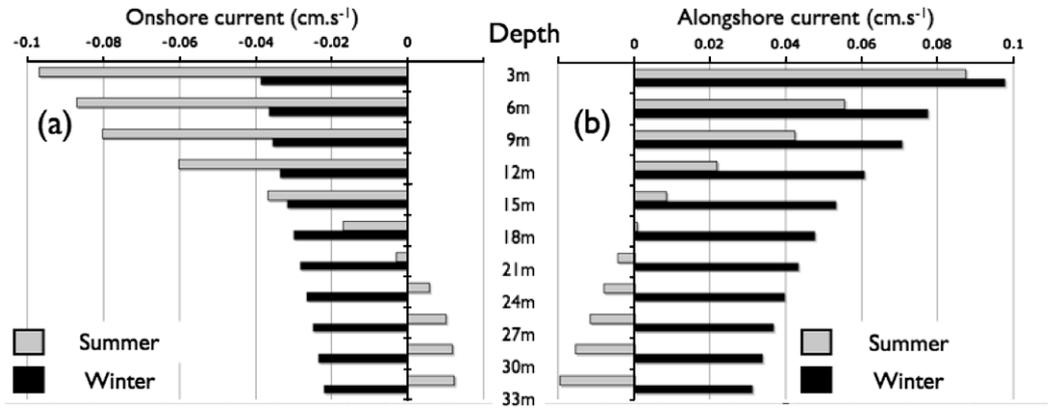
Fig. 10. Average vertical structure (0–30 m) of the flow obtained from the climatological hydrodynamic model simulations (one year) in summer and in winter from 6°S to 14°S over the coastal area (until isobath 2200 m). (a) Onshore current and (b) Alongshore current component. In summer there is a current shear around 20 m that doesn't appear in winter.

3.2.3. Spatio-temporal pattern

We plotted similar Hovmuller representations for both anchovy egg concentrations (field data) and retention values derived from Simulation III with a 15 m depth scenario (Fig. 9). The field data showed a spawning summer peak from 6°S to 10°S, while the model indicated a summer maximum of retention further south at 14°S–16°S. There was a winter spawning peak from 7°S to 12°S and at 18°S, which roughly matched peaks in retention. There was a high simulated retention for eggs released south of 18°S from May to September, but not enough field data allowed to make a comparison, although there was also maximum egg concentrations at 18°S in August. In both egg concentration data and simulated retention values, the summer peak was shorter than the winter peak, and values were low from March to May all along the domain.

4. Discussion

In temperate neritic waters the majority of pelagic fish eggs are spawned at shallow depths (<50 m) and are neutrally or slightly positively buoyant (Sundby, 1991). Our first experiment (Simulation I) consisted in releasing virtual eggs at three depth levels between 0 and 45 m depth all along the Peruvian coast, and considering larvae as retained if they were still in this area after a drifting period of 30 days. Spatially, there were two retention minimums (Fig. 2) corresponding to the abrupt changes in coastal orientation off Punta Falsa (2°S–6°S) and off Paracas (14°S–16°S, Fig. 1). Lett et al. (2007a) used a different criterion for retention, based on the distance traveled by particles from their initial positions, and found maximum retention in summer. Differences in these results are due to currents being more alongshore in winter, which resulted in particles being transported away from their original locations but remaining in the coastal area (Fig. 10b), so that particles were considered as retained by our retention criterion but not by Lett et al.'s (2007a). This was checked by running the simulations described here with both criteria for comparison. Bakun (1987) showed that while the volume of Ekman transport off Peru is much larger in winter, the rate of larval offshore transport is higher in summer. He explained this counter-intuitive result by pointing out that "drifting organisms which are distributed through the upper mixed layer would experience a faster net offshore drift in the thinner surface mixed layer of austral summer than in the deeper mixed layer of winter, even though the winter transport (by volume) is much larger". Our results agree with this theory, since on average we obtain better retention rates during winter. However, this pattern is sensitive to the spawning depth and location within the upwelling area, and in particular show a summer maximum of retention for particles released between 30 and 45 m (Fig. 3). This maximum occurs because the summer mixed layer is shallower and the offshore Ekman transport layer thinner, with onshore return currents as shallow as 25 m (Fig. 10a).

Spawning frequency and patchiness were not significant factors in the simulations, showing that the non-uniformity in the temporal and spatial distribution of egg release had no effect on retention. Regarding frequency, it might be due to the fact that we used monthly averaged forcing for the hydrodynamic model, which did not allow reproducing significant circulation variability within a month. Regarding patchiness, the null effect could mean that with a patchy spawning, after a short time of drift the eggs were so mixed all along the coast by the mesoscale structures that the final results did not significantly differ from a uniform initial distribution. Clearly these factors would be more important if small-scale biological factors like predation or feeding were included.

Since the currents displayed vertical shears near the surface in the upwelling area (Penven et al., 2005), the vertical distribution of eggs and larvae was a main factor affecting coastal retention. Generally, the factors likely to determine the vertical profile of pelagic fish eggs are spawning depth, buoyancy, vertical mixing, and depth-dependent mortality (Sundby, 1997). Typically, pelagic fish eggs accumulate at the sea surface and decrease in concentration exponentially with depth (Sundby, 1983). In the Bay of Biscay, Coombs et al. (2004) found eggs of both sardine and anchovy predominantly in the upper 20 m of the water column above the pycnocline, increasing in abundance towards the surface. This distribution is expected for buoyant particles under the influence of wind mixing at the surface, by considering the balance of the egg ascent and vertical diffusion (Sundby, 1991), and is consistent with other field reports (Coombs et al., 2003; Dopolo et al., 2005; Olivar et al., 2001). Observations in the northern Humboldt (7°S) for anchovy eggs showed a similar pattern (Ayón, 2004).

In Simulation II we used egg densities ranging from 1.023 to 1.027 $g\,cm^{-3}$. For a value of 1.023 $g\,cm^{-3}$, buoyancy was positive within the entire spawning area, while for both densities of 1.024 and 1.025 $g\,cm^{-3}$, part of the eggs ended up near the surface and another part (spatially segregated) accumulate around 40–50 m, probably near the pycnocline. For 1.026 and 1.027 $g\,cm^{-3}$, eggs sank below 50 m. These results suggest that egg densities leading to the typical observed vertical distribution are between 1.024 and 1.025 $g\,cm^{-3}$. Measurements of egg densities for *Engraulis ringens* are not available. Measurements for *Engraulis encrasicolus* in the Bay of Biscay gave an egg density around 1.023 $g\,cm^{-3}$ and a marked increase in density amounting to 1.025 $g\,cm^{-3}$ in the final quarter of egg development (Coombs et al., 2004). Simulation II also showed that coastal retention increased with egg density. Positive buoyancy of particles led to reduced retention because offshore transport was always faster near the surface. Other simulations (not presented) showed that various spawning depths (0–15, 15–30 or 30–45 m) had no significant effect on retention when the buoyancy scheme was included. We conclude that water density and pycnocline depth are significant parameters for determining egg coastal retention. The incubation time might also be important, since it determines the time during which eggs are exposed to the low retention rates occurring near the surface.

The vertical distribution of larvae is influenced by the same physical factors as for eggs but with the additional variable of swimming. Off Peru anchoveta larvae are typically found deeper than eggs, near the thermocline (Palomera and Sabatés, 1990; Sanchez et al., 1999; Shelton and Hutchings, 1979). Depending on the size of the larvae, they accumulate near the thermocline (Matsuura and Kitahara, 1995), or perform vertical migration between the surface and the thermocline (Shelton and Hutchings, 1979). In the Humboldt upwelling system, oxygen concentrations below 1 ml/l limit the depth of anchovy larvae (Morales et al., 1996) and adults (Mathisen, 1989). As the oxycline is usually found at the base of the thermocline in the central Humboldt (Morales et al., 1999), vertical swimming behavior might be limited by both

the thermocline and the oxycline. Preliminary studies of the vertical distributions of anchovy larvae in the northern Humboldt (at 7°S) suggest that they concentrate near the thermocline, between 30 and 50 m depth (Ayón, 2004).

Simulation III investigated the effect of different larval depth-regulatory behaviors: target depths of 1, 15 or 30 m and diurnal vertical migration (DVM) from 1 to 30 m, with age-dependent larval swimming velocities. We found that DVM and a constant depth of 15 m produced similar patterns of retention, typically with retention peaks in winter and summer. Constant 1 and 30 m depth regulation produced opposite seasonal patterns: at 1 m it was maximal while at 30 m it was minimal in winter. This is understandable by looking at the average vertical structures of the flows from the surface to 30 m depth in summer and in winter (Fig. 10). At the surface, during winter, the offshore component of the currents is weaker, leading to a better coastal retention. At 30 m depth currents flow onshore in summer, which also leads to increased retention. The thermocline is shallower during summer and deeper in winter, so that eggs and larvae might be more confined to surface waters during summer. Taking this into account would increase larval retention in winter. Carr et al. (2008) performed DVM modeling experiments in the Californian current system, and showed that the offshore transport experienced by individuals near surface during the night is not compensated by the subsurface onshore flow where individuals migrate during the day time, which is also consistent with Fig. 10.

The sensibility test on lethal temperature showed that temperature is probably not a limiting factor for anchovy early life survival, at least in the climatological case. Of course the actual effect of cold is to slow swimming and growth and indirectly increase mortality rates, but our results show that eggs and larvae usually do not experience temperatures lower than the optimal expected for larval survival. This optimum is given in the literature as being intermediate in the observed temperature range for adults anchovy spawning, which is 14–21 °C in this region (Jarre et al., 1991; Llanos-Rivera and Castro, 2006; Pauly and Soriano, 1989).

Upwelling-favorable wind is generally maximal in winter (Bakun, 1987; Lett et al., 2007a). Chlorophyll displays a first maximum in spring then peaks in summer (Carr and Kearns, 2003; Thomas et al., 2004). Zooplankton concentration peaks in spring (Carrasco and Lozano, 1989). Although anchovy eggs are found all around the year in the northern Humboldt upwelling area, there are usually two peaks of spawning (summer and winter) with winter being much more significant (Fig. 7; Santander, 1981). However, literature (Senocak et al., 1989) and year by year data analysis indicated that the spatio-temporal spawning patterns also showed interannual as well as interdecadal changes, affecting the locations of spawning and the relative intensities of the two spawning peaks. The reason why the major anchovy spawning peak does not coincide with the plankton peak is unclear.

Anchovy eggs are found mostly from the coast to the 100 m isobath, with the greatest abundances from 6°S to 14°S (Ayón et al., 2004), where the continental shelf is wide (Fig. 1). However, our model indicated that coastal retention should be higher from 8°S to 14°S than from 6°S to 8°S, suggesting that eggs spawned south of 8°S may have better chances of survival (Fig. 8). This is consistent with other findings showing that the best conformity between egg abundance and recruitment was between 10°S and 14°S (Einarsson and Rojas de Mendiola, 1966). From 3°S to 6°S little spawning is generally observed. The simulated retention rates were low in this region throughout the year (Fig. 9). This might reflect adaptive behavior to avoid offshore transport of eggs, but also could occur because this area is the limit between warm equatorial waters and cold waters from the coastal upwelling, and is not always suitable anchoveta habitat. In the southern part of the domain, from 14°S to 20°S the model retention rates were good but

observed egg concentrations are low. This apparent conflict might be related to the very narrow continental shelf in this region, which could limit the number of spawners in that area or cause the model to overestimate retention.

The existence of two seasons and places of best retention could lead to the existence of multiple anchoveta populations, as suggested by Mathisen (1989). However, the fact that spawning occurs throughout the year lessens the likelihood of functional allopatry and may reflect bet-hedging strategy of the older year-classes, as suggested by McQuinn (1997) in the case of herring. In this case the older anchovy classes, being more fecund, could have a protracted spawning season (wave spawning), as a bet-hedging strategy in a variable environment (Lambert and Ware, 1984; McQuinn, 1997; Muck, 1989). Larval retention rates suggest better larval survival in summer and winter (our results), and generate the corresponding reproduction peaks in the following year with a positive feed-back. The fact that immature fish, spawned six months earlier, dominate the catch in summer while in winter the total biomass is dominated by mature fish (Mathisen, 1989) suggest that winter spawning leads to a more successful recruitment, which is consistent with the maximum modeled retention success for spawning in winter in the 0–100 m area.

Our simulations produced impartial and robustness results. Nevertheless, we have to stress the limitations of the present study. The hydrodynamic model reproduces the mean seasonal circulation and eddy activity, but does not reproduce the strong inter-annual variability, characteristic of the northern Humboldt in relation with ENSO events (Mackas et al., 2006; Strub et al., 1998). The role of these events on the reproductive success are likely important and will be explored when adequate interannual simulations become available and validated. Moreover, although coastal retention is probably important for larval survival, other important more direct factors like food availability and predation need to be considered. In a first attempt to try to match (1) retention indices derived from a model and (2) IMARPE egg concentration data for anchovy, we adopted the principle of the pattern-oriented modelling approach proposed by Grimm et al. (2005). That approach focused on modeling general pattern rather than on a quantitative estimation of egg-to-anchoveta production. It is difficult to make such quantitative comparisons for many reasons: the modeled and observed quantities compared are not the same, the time series used have different durations, the variability of the datasets are different, etc. However, a qualitative comparison is useful. "Useful patterns need not be striking; qualitative or "weak" patterns can be powerful in combination." (Grimm et al., 2005). Here we used a combination of spatial and seasonal patterns.

A similar modeling methodology has been applied in the Benguela Current system to investigate the dynamics of anchovy (*Engraulis encrasicolus*) and sardine (*Sardinops sagax*) ichthyoplankton. Stenevik et al. (2003) used for sardine in the northern Benguela off Namibia an approach similar to ours. Indeed, because spawning and nursery areas are overlapping in both cases, the main process investigated was retention. In contrast, in the southern Benguela off South Africa, anchovy spawning and nursery areas are about 500 km apart. Therefore, transport between spawning and nursery areas was the process under focus (Huggett et al., 2003). This is less clear for sardine in the southern Benguela, and both transport and retention were considered (Miller et al., 2006). It was shown that egg buoyancy was a determining factor for transport in the southern Benguela (Parada et al., 2003). In the northern Humboldt, we found that this factor was also key for egg retention. In the Benguela, temperature appeared to be an important parameter for ichthyoplankton survival (Lett et al., 2007b; Mullon et al., 2003), but this is not the case in the Canary current system (Brochier et al., 2008), nor in the northern Humboldt as our results suggest. We

must however keep in mind that we used climatological hydrodynamic simulations; during a "la niña" episode, the lower sea temperature could limit egg and larval development. Regarding spawning temporal pattern, there is in the southern Benguela one seasonal peak for anchovy and two peaks for sardine (van der Lingen and Huggett, 2003). There are indications that these peaks are related with good transport (Huggett et al., 2003), enrichment and retention (Lett et al., 2006; Miller et al., 2006) conditions in the respective spawning and nursery areas, as we also found for the two spawning peaks of anchovy in the northern Humboldt.

In conclusion, considering only a Lagrangian drift, spawning at different depths (but not frequency, nor patchiness) strongly influenced retention rates (Simulation I); the egg density (Simulation II) and swimming behavior of larvae (Simulation III) also affected the retention rates. In future, we would like to use interannual hydrodynamic simulations to observe ENSO's effects on larval anchoveta early life. This could be done by using a coupled biophysical–biogeochemical model to reproduce the oxygen minimum depth and larval food fields that could enable us to better characterize good recruitment conditions. Finally, it would be interesting to incorporate the effect of small-scale turbulence on larval transport and mortality in the model (Guizien et al., 2006; Lasker et al., 1978; MacKenzie, 2000; Sundby, 1997).

References

Ayón, P., 2004. Informe AEPS Crucero demersales 1994–2004. IMARPE.
Bakun, A., 1987. Monthly variability in the ocean habitat off Peru deduced from maritime observations, 1953–1984. In: Pauly, D., Tsukayama, I. (Eds.), The Peruvian Anchoveta and its Upwelling Ecosystems: Three Decades of Change. ICLARM Studies and Reviews, pp. 46–74.
Bakun, A., 1996. Patterns in the ocean. Ocean processes and marine population dynamics. University of California Sea Grant, California, USA, in cooperation with Centro de Investigaciones Biologicas de Noroeste, La Paz, Baja California Sur, Mexico, 323 pp.
Batteen, M.L., 1997. Wind-forced modeling studies of currents, meanders, and eddies in the California Current System. Journal of Geophysical Research 102, 985–1010.
Bertrand, A., Segura, M., Gutiérrez, M., Vásquez, L., 2004. From small-scale habitat loopholes to decadal cycles: a habitat-based hypothesis explaining fluctuation in pelagic fish populations off Peru. Fish and Fisheries 5 (4), 296–316.
Brochier, T., Ramzi, A., Lett, C., Machu, E., Fréon, P., Hernández-León, S., 2008. Modelling the biophysical dynamics of sardine and anchovy ichthyoplankton in the Canary Upwelling System. Journal of Plankton Research 30, 1133–1146.
Carr, M.E., Kearns, E.J., 2003. Production regimes in four Eastern Boundary Current systems. Deep-Sea Research Part II – Topical Studies in Oceanography 50 (22–26), 3199–3221.
Carr, S.D., Capet, X.J., McWilliams, J.C., Pennnington, J.T., Chavez, F.P., 2008. The influence of diel vertical migration on zooplankton transport and recruitment in an upwelling region: estimates from a coupled behavioral-physical model. Fisheries Oceanography 17 (1), 1–15.
Carrasco, S., Lozano, O., 1989. Seasonal and long-term variations of zooplankton volumes in the Peruvian Sea, 1964–1987. In: Pauly, D., Muck, P., Mendo, J., Tsukayama, I. (Eds.). The peruvian Upwelling Ecosystem: Dynamics and Interactions. Instituto del Mar del Peru (IMARPE), Peru, pp. 82–85.
Castro, L.R., Hernández, E.H., 2000. Early life survival of the anchoveta Engraulis ringens off central Chile during the 1995 and 1996 winter spawning seasons. Transactions of the American Fisheries Society 129 (5), 1107–1117.

Coombs, S.H., Boyra, G., Rueda, L.D., Uriarte, A., Santos, M., Conway, D.V.P., Halliday, N.N., 2004. Buoyancy measurements and vertical distribution of eggs of sardine (*Sardina pilchardus*) and anchovy (*Engraulis encrasicolus*). Marine Biology 145 (5), 959–970.

Coombs, S.H., Giovanardi, O., Halliday, N.C., Franceschini, G., Conway, D.V.P., Manzueto, L., Barrett, C.D., McFadzen, I.R.B., 2003. Wind mixing, food availability and mortality of anchovy larvae *Engraulis encrasicolus* in the northern Adriatic Sea. Marine Ecology Progress Series 248, 221–235.

Cury, P., Bakun, A., Crawford, R.J.M., Jarre, A., Quiñones, R.A., Shannon, L.J., Verheye, H.M., 2000. Small pelagics in upwelling systems: patterns of interaction and structural changes in "wasp-waist" ecosystems. Ices Journal of Marine Science 57 (3), 603–618.

Cury, P., Roy, C., 1989. Optimal environmental window and pelagic fish recruitment success in upwelling areas. Canadian Journal of Fisheries and Aquatic Sciences 46, 670–680.

Dopolo, M., Van der Lingen, C., Moloney, C., 2005. Stage-dependent vertical distribution of pelagic fish eggs on the western Agulhas Bank, South Africa. African Journal of Marine Science 27, 249–256.

Einarsson, H., Rojas de Mendiola, B., 1966. An attempt to estimate annual spawning intensity of the anchovy (*Engraulis ringens* jenyns) by means of regional egg and larval survey during 1961–1964. Report volume XI.

Fogarty, M.J., 1993. Recruitment in randomly varying environments. ICES Journal of Marine Science 50, 247–260.

Fréon, P., Alheit, J., Barton, E.D., Kifani, S., Marchesiello, P., 2006. Modelling, forecasting and scenarios in comparable upwelling ecosystems: California, Canary and Humboldt. In: Hempel, G., Moloney, C., Rizzoli, P., Woods, J. (Eds.). The Benguela: Predicting a Large Marine Ecosystem. Elsevier Series, Large Marine Ecosystems.

Fréon, P., Cury, P., Shannon, L., Roy, C., 2005. Sustainable exploitation of small pelagic fish stocks challenged by environmental and ecosystem changes: a review. Bulletin of Marine Science 76 (2), 385–462.

Grimm, V., Berger, U., Bastiansen, F., Eliassen, S., Ginot, V., Giske, J., Goss-Custard, J., Grand, T., Heinz, S.K., Huse, G., Huth, A., Jepsen, J.U., Jørgensen, C., Mooij, W.M., Müller, B., Pe'er, G., Piou, C., Railsback, S.F., Robbins, A.M., Robbins, M.M., Rossmanith, E., Ruger, N., Strand, E., Souissi, S., Stillman, R.A., Vabø, R., Visser, U., DeAngelis, D.L., 2006. A standard protocol for describing individual-based and agent-based models. Ecological Modelling 198, 115–126.

Grimm, V., Railsback, S.F., 2005. Individual-Based Modeling and Ecology. Princeton University Press, Princeton, NJ.

Grimm, V., Revilla, E., Berger, U., Jeltsch, F., Mooij, W.M., Railsback, S.F., Thulke, H.-H., Weiner, J., Wiegand, T., DeAngelis, D.L., 2005. Pattern-oriented modeling of agent-based complex systems: lessons from ecology. Science 310, 987–991.

Guizien, K., Brochier, T., Duchêne, J., Koh, B., Marsaleix, P., 2006. Dispersal of *Owenia fusiformis* larvae by wind-driven currents: turbulence, swimming behaviour and mortality in a three-dimensional stochastic model. Marine Ecology Progress Series 311, 47–66.

Haidvogel, D.B., Beckmann, A., 1998. Numerical modeling of the coastal ocean. In: Brink, K.H., Robinson, A.R. (Eds.). The Sea, vol. 10. Harvard University Press, Cambridge, pp. 457–482.

Huggett, J., Fréon, P., Mullon, C., Penven, P., 2003. Modelling the transport success of anchovy *Engraulis encrasicolus* eggs and larvae in the southern Benguela: the effect of spatio-temporal spawning patterns. Marine Ecology Progress Series 250, 247–262.

Hunter, J.R., 1977. Behavior and survival of northern anchovy *Engraulis Mordax* larvae. California Cooperative Oceanic Fisheries Investigations Reports 19, 138–146.

Jacobson, L.D., De Oliveira, J.A.A., Barange, M., Cisneros-Mata, M.A., Félix-Uraga, R., Hunter, J.R., Kim, J.Y., Matsuura, Y., Ñiquen, M., Porteiro, C., Rothschild, B., Sanchez, R.P., Serra, R., Uriarte, A., Wada, T., 2001. Surplus production, variability, and climate change in the great sardine and anchovy fisheries. Canadian Journal of Fisheries and Aquatic Sciences 58 (9), 1891–1903.

Jarre, A., Muck, P., Pauly, D., 1991. Two approaches for modelling fish stock interactions in the Peruvian upwelling ecosystem. Multispecies Models Relevant to Management of Living Resources, Copenhagen, Denmark, pp. 171–184.

Lambert, T., Ware, D.M., 1984. Reproductive strategies of demersal and pelagic spawning fish. Canadian Journal of Fisheries and Aquatic Sciences 41 (11), 1565–1569.

Lasker, R., 1985. What limits clupeoid production? Canadian Journal of Fisheries and Aquatic Sciences 42 (Suppl. 1), 31–38.

Lasker, R., Parsons, T.R., Jansson, B.O., Longhurst, A.R., Saetersdal, G. (Eds.), 1978. The Relation between Oceanographic Conditions and Larval Anchovy Food in the California Current: Identification of Factors Contributing to Recruitment Failure.

Lett, C., Penven, P., Ayón, P., Fréon, P., 2007a. Enrichment, concentration and retention processes in relation to anchovy (*Engraulis ringens*) eggs and larvae distributions in the northern Humboldt upwelling ecosystem. Journal of Marine Systems 64, 189–200.

Lett, C., Veitch, J., van der Lingen, C.D., Hutchings, L., 2007b. Assessment of an environmental barrier to transport of ichthyoplankton from the southern to the northern Benguela ecosystems. Marine Ecology- Progress Series 347, 247–259.

Lett, C., Rose, K.A., Megrey, B.A., in press. Biophysical models. In: Checkley, D.M., Alheit, J., Oozeki, Y., Roy, C. (Eds.). Climate Change and Small Pelagic Fish, Cambridge University Press (Chapter 6).

Lett, C., Roy, C., Levasseur, A., van der Lingen, C.D., Mullon, C., 2006. Simulation and quantification of enrichment and retention processes in the southern Benguela upwelling ecosystem. Fisheries Oceanography 15, 363–372.

Lett, C., Verley, P., Mullon, C., et al., 2008. A Lagrangian tool for modelling ichthyoplankton dynamics. Environmental Modelling & Software 28, 1210–1214.

Llanos-Rivera, A., Castro, L.R., 2006. Inter-population differences in temperature effects on Engraulis ringensyolk-sac larvae. Marine Ecology Progress Series 312, 245–253.

Mackas, D.L., Strub, P.T., Thomas, A.C., Montecino, V., 2006. Eastern Ocean Boundaries Pan Regional. In: Brink, K.H., Robinson, A.R. (Eds.). The Sea, vol. 14A. Harvard University Press, Cambridge (Chapter 2).

MacKenzie, B.R., 2000. Turbulence, larval fish ecology and fisheries recruitment: a review of field studies. Oceanologica Acta 23 (4), 357–375.

Marchesiello, P., McWilliams, J.C., Shchepetkin, A., 2003. Equilibrium structure and dynamics of the California Current System. Journal of Physical Oceanography 33, 753.

Mathisen, O.A., 1989. Adaptation of the anchoveta (*Engraulis ringens*) to the Peruvian upwelling system. In: Pauly, D., Muck, P., Mendo, J., Tsukayama, I., (Eds.). The Peruvian Upwelling Ecosystem: Dynamics and Interactions. ICLARM Conference Proceedings, pp. 220–234.

Matsuura, Y., Kitahara, E.M., 1995. Horizontal and vertical distribution of anchovy *Engraulis anchoita* eggs and larvae off Cape Santa Marta Grande in southern Brazil. Archive of Fishery and Marine Research 42 (3), 239–250.

McQuinn, I.H., 1997. Metapopulations and the Atlantic herring. Reviews in Fish Biology and Fisheries 7, 297–329.

Miller, D.C.M., Moloney, C.L., van der Lingen, C.D., Lett, C., Mullon, C., Field, J.G., 2006. Modelling the effects of physical–biological interactions and spatial variability in spawning and nursery areas on transport and retention of sardine Sardinops sagax eggs and larvae in the southern Benguela ecosystem. Journal of Marine Systems 61, 212–229.

Miller, T.J., 2007. Contribution of individual-based coupled physical biological models to understanding recruitment in marine fish populations. Marine Ecology Progress Series 347, 127–138.

Morales, C.E., Braun, M., Reyes, H., Blanco, J.L., Davies, A.G., 1996. Anchovy larval distribution in the coastal zone off northern Chile: the effect of low dissolved oxygen concentrations and of a cold-warm sequence (1990–95). Investigaciones Marinas 24, 77–96.

Morales, C.E., Hormazabal, S.E., Luis Blanco, J., 1999. Interannual variability in the mesoscale distribution of the depth of the upper boundary of the oxygen minimum layer off northern Chile (18–24S): implications for the pelagic system and biogeochemical cycling. Journal of Marine Research 57, 909–932.

Muck, P., 1989. Relationships between anchoveta spawning strategies and the spatial variability of sea surface temperature off Peru. In: Workshop on Models for Yield Prediction in the Peruvian Ecosystem, Callao (Peru) 24–28 August 1987, ICLARM Conference Proceedings, pp. 168–173.

Mullon, C., Freon, P., Parada, C., van der lingen, C., Huggett, J., 2003. From particles to individuals: modelling the early stages of anchovy (*Engraulis capensis/ encrasicolus*) in the southern Benguela. Fisheries Oceanography 12 (4/5), 396–402.

Myers, R.A., 1998. When do environment-recruitment correlations work? Reviews in Fish Biology and Fisheries 8 (3), 285–305.

Myers, R.A., Bowen, K.G., Barrowman, N.J., 1999. Maximum reproductive rate of fish at low population sizes. Canadian Journal of Fisheries and Aquatic Sciences 56, 2404–2419.

Ñiquen, M., Fréon, P., 2006. A new record set by the Peruvian fishery 2.5 million tonnes of anchovy landed in November 2005. GLOBEC International Newsletter, 56–57.

Olivar, M.P., Salat, J., Palomera, I., 2001. Comparative study of spatial distribution patterns of the early stages of anchovy and pilchard in the NW Mediterranean Sea. Marine Ecology Progress Series 217, 111–120.

Palomares, M.L., Muck, P., Mendo, J., Chuman, E., Gomez, O., Pauly, D., 1987. Growth of the Peruvian anchoveta (*Engraulis ringens*), 1953–1982. In: Pauly, D., Tsukayama, I. (Eds.), The Peruvian Anchoveta and its Upwelling Ecosystems: Three Decades of Change. ICLARM Studies and Reviews, Berlin, pp. 117–141.

Palomera, I., Sabatés, A., 1990. Co-occurence of Engraulis encrasicolus and Sardinella aurita eggs and larvae in the northwestern Mediterranean. Scientia Marina 54 (1), 61–67.

Parada, C., van der Lingen, C.D., Mullon, C., Penven, P., 2003. Modelling the effect of buoyancy on the transport of anchovy (*Engraulis capensis*) eggs from spawning to nursery ground in the southern Benguela: an IBM approach. Fisheries Oceanography 12 (3), 170–184.

Pauly, D., Soriano, M., 1989. Production and mortality of anchoveta (*Engraulis ringens*) eggs off Peru. In: Pauly, D., Muck, P., Mendo, J., Tsukayama, I. (Eds.). The Peruvian Upwelling Ecosystem: Dynamics and Interactions, pp. 155–167.

Penven, P., Echevin, V., Pasapera, J., Colas, F., Tam, J., 2005. Average circulation, seasonal cycle, and mesoscale dynamics of the Peru Current System: a modeling approach. Journal of Geophysical Research 110, C10021.

Sanchez, R.P., Ciechomski, J.D., Lasta, C., Guerrero, R., 1999. A drift study of vertical distribution and mortality of *Engraulis anchoita* eggs and larvae. Revista de Investigacion Desarrollo Pesquero 12, 51–75.

Santander, H., 1981. Distribution patterns and fluctuations in anchovy and sardine spawning. 0378-7699, Callao.

Senocak, T., Schnack, D., Pauly, D., 1989. Mean monthly distribution, abundance and production of anchoveta eggs off Peru (4°S –14°S), 1964–1971 and 1972–1986. In: Pauly, D., Muck, P., Mendo, J., Tsukayama, I. (Eds.). The Peruvian Upwelling Ecosystem: Dynamics and Interactions. ICLARM Conference Proceedings, pp. 143–154.

Shchepetkin, A.F., McWilliams, J.C., 2005. The regional oceanic modeling system (ROMS): a split-explicit, free-surface, topography-following-coordinate oceanic model. Ocean Modelling 9 (4), 347–404.

Shelton, P.A., Hutchings, L., 1979. The Effect of the Environment on Spawning and Recruitment in the Anchovy (Engraulis capensis Gilchrist) ICES Symposium on the Early Life History of Fish. Woods Hole, MA (USA).

Stenevik, E.K., Skogen, M., Sundby, S., Boyer, D., 2003. The effect of vertical and horizontal distribution on retention of sardine (*Sardinops sagax*) larvae in the Northern Benguela – observations and modelling. Fisheries Oceanography 12 (3), 185–200.

Strub, P.T., Mesias, V., Montecino, V., Ruttland, J., Salinas, S., 1998. Coastal ocean circulation off Western South America. The Sea, 11.

Sundby, S., 1983. A one-dimensional model for the vertical distribution of pelagic fish eggs in the mixed layer. Deep-Sea Research 30, 645–661.

Sundby, S., 1991. Factors affecting the vertical distribution of eggs. In: ICES Marine Science Symposia, pp. 33–38.

Sundby, S., 1997. Turbulence and ichthyoplankton: influence on vertical distributions and encounter rates. Scientia Marina 61 (1), 159–176.

Thomas, A.C., Strub, P.T., Carr, M.E., Weatherbee, R., 2004. Comparisons of chlorophyll variability between the four major global eastern boundary currents. International Journal of Remote Sensing 25 (7–8), 1443–1447.

van der Lingen, C.D., Huggett, J.A., 2003. The role of ichthyoplankton surveys in recruitment research and management of South African anchovy and sardine. In: Browman, H.I., Skiftesvik, A.B. (Eds.), The Big Fish Bang. Proceedings of the 26th Annual Larval Fish Conference. Institute of Marine Research, Bergen, Norway, pp. 303–343.

Walsh, J.J., Whitledge, T.E., Esaias, W.E., Smith, R.L., Huntsman, S.A., Santander, H., Rojas de Mendiola, B., 1980. The spawning habitat of the Peruvian anchovy, *Engraulis ringens*. Deep-Sea Research 27A, 1–27.

Ware, D.M., Rojas de Mendiola, B., Newhouse, D.S., 1980. Behaviour of first-feeding Peruvian anchovy larvae, *Engraulis ringens* J. In: Sherman, K., Hempel, G. (Eds.). Symposium on Early Life History of Fish. Conseil International pour l'Exploitation de la Mer, Rapport et procés-verbaux des réunions, pp. 80–87.

Werner, F.E., Quinlan, J.A., Lough, R.G., Lynch, D.R., 2001. Spatially-explicit individual based modeling of marine populations: a review of the advances in the 1990s. Sarsia 86 (6), 411–421.